Elementary excitations of C_{60} from the far infrared to the far vacuum ultraviolet studied by high-resolution electron-energy-loss spectroscopy

A. Lucas, G. Gensterblum, J. J. Pireaux, P. A. Thiry, R. Caudano, J. P. Vigneron, and Ph. Lambin
Facultés Universitaires Notre-Dame de la Paix, 61 rue de Bruxelles, B-5000 Namur, Belgium

W. Krätschmer
Max Planck Institut für Kernphysik, P.O. Box 103980, D-6900 Heidelberg 1, Federal Republic of Germany
(Received 26 September 1991)

We report on measurements by high-resolution electron-energy-loss spectroscopy (HREELS) of the excitation spectrum of thin films of C_{60} (containing less than 10% of C_{70}) deposited onto Si(100) in ultrahigh vacuum. Most of our spectra have been taken in the specular direction of the reflected beam. By varying the primary-electron energy from 2 to 150 eV, the frequency regions extending from the far ir, through the visible-uv, to the far vuv have been investigated on one single specimen in the same spectrometer with a resolution varying from 10 meV in the ir to 60 meV in the vuv. Since no strict selection rules apply to electron inelastic scattering, the present data contain information on many of the elementary excitations of the C_{60} fullerite film. Several of the spectral features are comparable to the observations of photon, photoelectron, and neutron spectroscopies which address separate parts of the spectrum. Important additional features are revealed by HREELS, including a transition at 1.55 eV which appears to be the lowest one-electron excitation observed in C_{60} and two collective excitations at 6.3 eV (π plasmons) and 28 eV (σ plasmons). When possible, the band intensities are discussed with the help of the dielectric theory of EELS. The present data further advance our knowledge of the rich spectrum of elementary vibrational and electronic excitations of the C_{60} fullerite.

I. INTRODUCTION

Since the discovery of the spherical, hollow carbon cluster C_{60} fullerene[1] and especially since the recent development of methods[2] for its synthesis in large amounts, this and other molecules of the so-called fullerene family have quickly gained the status of a paradigm in physical chemistry.[3] There is such a great interest in this state of elemental carbon matter that, in less than a year, nearly all available spectroscopic techniques have already been brought to bear on the elucidation of the vibrational, electronic, and other properties of the molecules in their gaseous and condensed states.

The purpose of the present paper is to report on spectroscopic results on C_{60} obtained by high-resolution electron-energy-loss spectroscopy (HREELS). There are many advantages to this method[4] for the study of gases, solids, and their surfaces, particularly its ability to cover in a single experiment the very broad range of frequencies extending from the far infrared (where the high resolution is required) to the soft-x-ray regimes. This enabled us to detect 11 infrared frequencies or groups of frequencies of the 46 distinct vibrational modes of the molecule and to observe 22 bound-bound and bound-free electronic resonances from 1.5 to 30 eV. Many of those have already been detected by other methods and we will endeavor to make a comparison of our data with already published ones. An additional transition at 1.55 eV is clearly revealed, which we believe to be the lowest-energy single-particle excitation of C_{60} observed. We have further proved that, like graphite, a single molecule is able to experience separate collective oscillations of its π-electron subsystem whose quanta occur near 6 eV (π plasmons). We have also confirmed the existence of a second, broader collective resonance, near 28 eV (σ plasmons), of the complete valence shell of the molecule. These plasmon resonances have been unambiguously identified via the peculiar sensitivity of their HREELS intensity to the primary-electron energy. We conclude the paper with a simple evaluation of the van der Waals cohesive energy of the C_{60} fullerite fcc crystal by attributing it, in principal order, to the dipolar interaction between the latter σ plasmons of $l=1$ symmetry on neighboring molecules.

II. EXPERIMENTAL DETAILS

The experiments were performed in a two-chamber UHV system equipped with a high-resolution electron spectrometer (Riber). The basis pressure in the analysis and preparation chambers was 5×10^{-11} and 1×10^{-8} Torr, respectively. The spectrometer consists of two 180° hemispherical electrostatic selectors, one acting as monochromator, the other as analyzer. The energy of the monochromatic electron beam can be varied from 0 up to 150 eV. It can be measured precisely by scanning the spectra up to the cutoff of the intensity. The energy resolution is 10 to 13 meV for the ir region and 0.04 to 0.06 eV for the visible and uv regions. The incident and collected beam directions are normally set at 45° to the normal and the spectrometer has a 1.5° half-angle aperture.

Carbon soot was produced by evaporation of graphite in an atmosphere at 100 Torr of helium.[2] The fullerenes

were extracted from the soot by solution with toluene. The resulting mixture contains approximately 85% C_{60} and 15% C_{70}. It was then sublimed at pressures of 6×10^{-8} Torr at ~300 °C and condensed onto a clean surface of Si(100) at room temperature. *In situ* cleaning of the Si(100) substrate prior to film deposition was performed by annealing at 1000 K. The vapor pressure of C_{70} being lower than that of C_{60}, the content of C_{70} in the thin films is expected to be less than 10%. For sublimation of the fullerenes we used a Knudsen cell with a boron-nitride crucible. The deposition rate was about 4 Å per minute. The thickness of the deposited film was estimated with a quartz-crystal oscillator to be about 60 Å. It had to be sufficiently small to avoid the typical charging effect on insulators when using a low-energy electron beam. On the other hand, it had to be large enough to eliminate the substrate-loss features. The Si(100) surface was chosen as a substrate instead of the often-used GaAs(110) surface because the former is optically inactive in the infrared range while the latter presents strong surface phonon-loss features in the range below 100 meV, which would certainly interfere with the C_{60} bands.

III. RESULTS AND DISCUSSION

In discussing the spectra, we have ascertained that one can ignore the contribution of C_{70} ($<10\%$) by checking on the known spectral properties of this molecule whenever additional peaks are present in the HREELS spectra as compared to data from other spectroscopies.

A. Infrared

Figure 1 shows the ir energy losses in the range of 25 meV to 0.5 eV with the sample at room temperature. The resolution was 10.5 meV. The gain spectrum is not shown, as it consists merely in a mirror image of the loss spectrum scaled down by the Boltzmann factor $\exp(-\hbar\omega/k_BT)$.[4]

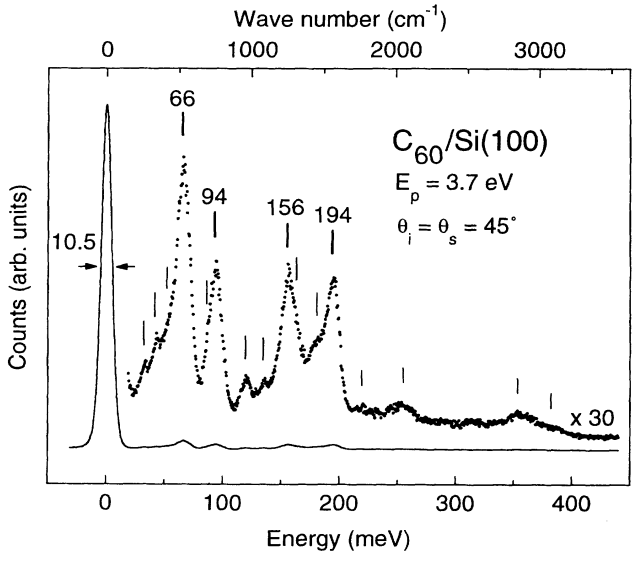

FIG. 1. HREELS spectrum of C_{60}-film/Si(100) in the infrared range. Peak positions are indicated by bars and are listed in Table I.

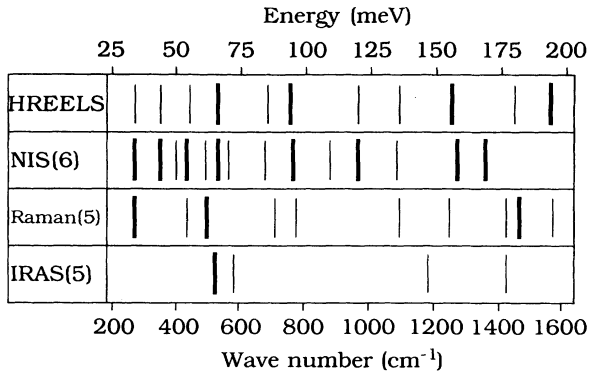

FIG. 2. Peak positions of ir bands of C_{60} as measured by four techniques. The acronyms stand for neutron inelastic scattering (NIS) and infrared absorption spectroscopy (IRAS). This figure is a graphical representation of the information in Table I. The strong features in each spectroscopy are indicate by a thick line.

From 25 to 200 meV there are 11 distinct peaks at frequencies which have been listed in Table I and Fig. 2, where they are compared with infrared-absorption-spectrum (IRAS),[5] Raman,[5] and neutron[6] spectroscopic

TABLE I. C_{60} ir bands. Comparative list of peak positions of ir bands observed in four different spectroscopies: HREELS, (neutron inelastic scattering) (NIS), Raman, and IRAS. The strong features are indicated by an asterisk and are represented by a thick line in Fig. 2 which provides a graphical representation of this table.

HREELS[a]		NIS[b]		Raman[c]	IRAS[c]
E (meV)	E (cm^{-1})	E (meV)	E (cm^{-1})	E (cm^{-1})	E (cm^{-1})
34	274	34	274*	273*	
44	355	44	355*		
		50	403		
55	444	54	436*	437	
		61	492	496*	
66	532*	66	532*		527*
		70	565		577
85	686	84	678		
				710	
94	758*	95	766*	774	
		109	879		
120	968	120	968*		
136	1097	135	1089	1099	
					1183
156	1258*			1250	
		158	1274*		
		169	1363*		
				1428	1428
180	1452				
				1470*	
194	1565*			1570	

[a]This work.
[b]Reference 6.
[c]Reference 5.

results. The sharpness of the ir bands in Fig. 1 is resolution limited. Comparison with theoretically calculated vibrational frequencies of C_{60} has already been made in Ref. 6 and will not be rediscussed. The most intense HREELS band centered at 66 meV (532 cm^{-1}) falls near the two strongest IRAS lines at 527 and 577 cm^{-1}, which are too close to be resolved here. From the dielectric theory of specular EELS,[4,7] one expects that the strong dipole-active modes should make a large contribution to the loss spectrum, especially in the presence of a substrate with a high ir dielectric constant such as Si, which enhances the dipole strength of vibrations perpendicular to the surface. This indeed appears to be the case for the 66-meV band. However, some strength in the low-energy side of this asymmetric band is likely to be due to the strong, Raman-active, radial-breathing A_g mode at 496 cm^{-1}. This mode can be efficiently electron excited by a Raman-like process, i.e., via the modulation imposed by the breathing motion to the multipolar polarizability of C_{60} and, hence, to the self-energy of the slow electron impacting on the molecule.

The other three intense HREELS bands around 94, 156, and 194 meV in Fig. 1 correlate better with dipole-inactive, Raman, or neutron lines than with the relatively weak IRAS lines at 1183 and 1428 cm^{-1}. The 1183-cm^{-1} line is hidden in the low-energy wing of the strong 156-meV (1258 cm^{-1}) HREELS band, whereas the 1428-cm^{-1} line seems to contribute, together with the 1470-cm^{-1} Raman line, to the weak 180-meV (1452 cm^{-1}) band to the left of the strong 194-meV (1565 cm^{-1}) HREELS peak. Inspection of Table I or Fig. 2 shows that the strong features in each of the four spectroscopies do not often coincide with intense features in the other three. Such differences in the spectra stem from the different scattering mechanisms of the four probes. For example, our two strong bands at 94 and 156 meV are also strong in neutron but not in IRAS, nor in Raman. As a second example, in the Raman spectrum of C_{60}, the 1470-cm^{-1} line which is assigned[5] to the totally symmetric, double-bond stretching mode (pentagon pinch mode) is by far the strongest Raman line whereas, at the corresponding 182-meV position in HREELS, there is only a weak band whose strength may be made of independent contributions from this pentagon pinch, the dipole-active mode at 180 meV, and possibly the bending mode of a small CH contamination. The neutron spectrum does now show any strong line in this region, either. A third striking example of differences between the four spectroscopies is the 194-meV (1565 cm^{-1}) line, which is one of the four strongest in our HREELS results but which remains undetected by the other three spectroscopies except possibly by Raman, which has a fairly weak line at 1570 cm^{-1}.

Apart from the 66-meV band discussed previously, we do not know exactly which modes or group of modes are responsible for the most intense HREELS bands. A qualitative indication as to the general nature of the carbon frame motions giving rise to these HREELS bands can perhaps be gained by examining the phonon-dispersion relations on a basal surface of crystalline graphite observed by the same HREELS technique.[8] Here, there are large densities of vibrational states around 58 meV, 90–100 meV, 155–175 meV, and 180–200 meV. We find it rather remarkable that these four frequency domains closely correspond to our four C_{60} strongest bands (Fig. 1), as if dense frequency concentrations of vibrational modes of a graphite layer survived when, as it were, the sheet is warped into the C_{60} spherical geometry. A comparison between neutron spectra from C_{60}, glassy carbon and graphite powder measured recently[9] corroborates this simple view.

The dielectric theory of HREELS (Ref. 7) indicates that it should be possible to discriminate optically active from inactive modes, i.e., long-range dipole scattering from "impact" or short-range scattering, by measuring the off-specular spectrum: *Provided that the molecules form a well-ordered film* on the surface, the off-specular spectrum should exclude dipole-active modes whose intensities quickly vanish outside a narrow, forward-scattering angular lobe around the specular (or Bragg) peak. Unfortunately, our sample showed no diffraction spots, implying that the film is highly disordered or clumped in small islands. In this case, electrons are elastically scattered in all directions by the disorder and can further suffer inelastic losses to vibrations, irrespective of the scattering direction. When two spectra were taken at 25° and 80° reflection angles (for a fixed 45° incidence angle), we found that the elastic-peak intensity was different, but not by orders of magnitude from the specular value, and that the two loss spectra (not shown here) were indeed very similar to the specular one shown in Fig. 1. Since this null result does not exclude substantial dipole strength in the observed bands, further measurements on well-ordered films must be undertaken and will be reported elsewhere.[10]

The last few broad and weak bands in the ir HREELS spectrum around 225, 255, and 355 meV are due to the combinations (66+156), (66+194 and 94+156), (156+194 and 2×194) of the four strong bands below 200 meV, respectively. The relatively clear band at 355 also receives a contribution from the bond-stretching motion of the CH contaminant.

Finally, we want to mention that by taking several ir HREELS spectra with primary electron energies varying from 2 up to 10 eV, some of the peak *intensities* (particularly the 180-meV peak) were observed to increase rather strongly.[10] We may attempt to link this phenomenon to the existence of large variations of the electronic density of states in the continuum of the C_{60}^- molecular ion such as clearly observed by Jost *et al.* in *Inverse Photoemission Spectroscopy*.[11] These so-called shape resonances are temporarily occupied by the primary electron and can lead to large enhancement of the excitation probability of selected molecular vibrations.[7] There are, however, several such resonances from 2 to 10 eV,[11] so that it is not clear why they would result in a monotonous increase of an inelastic cross section. Another interpretation of the phenomenon (which will be invoked for the uv and vuv collective modes below) could be the progressive squeezing into the narrow spectrometer aperture of the forward-scattering angular lobe caused by the optically active mode at 180 meV, making this mode apparently

more intense as the primary electron energy increases. Disentangling these two effects will necessitate detailed measurements of the line shapes as a function of primary energy.[10]

B. Near ir-visible-ultraviolet

Turning now to the visible range, Fig. 3 shows a spectrum taken in the specular direction with primary electrons of 10 eV (resolution: 40 meV). First, note that in the wing of the elastic peak at low magnification, one clearly recognizes the two groups of far-ir strong bands discussed before around 0.1 and 0.2 eV, and also the weaker 0.36-eV combination and CH contamination band. At high magnification, still in the wing of the quasielastic peak, there are two rather sharp features at 0.55 and 0.71 eV. These can be interpreted, respectively, as the $0.2+0.36$ combination band and the 2×0.36 combination and double excitation of the CH stretch. This interpretation is supported by a quantitative evaluation of the respective intensities, using the Poisson statistics applicable to the multiple loss processes in HREELS.[7,12]

Further up in energy, there is a broad spectral region extending from 0.8 to 1.4 eV which is absolutely free of any feature in a background of extremely low noise intensity. This gap in the excitation spectrum is followed by a sharp onset at 1.45 eV and a very clear peak at 1.55 eV. We believe we are observing here at high resolution, the accurate value of an electronic excitation in C_{60}. As pointed out by Jost *et al.*,[11] because of excitonic effects, this need not coincide with the highest occupied molecular orbital–lowest unoccupied molecular orbital level separation theoretically predicted at 1.7 eV,[13] nor with the C_{60} fullerite band gap calculated at 1.5 eV.[14] Note that C_{70} has very nearly the same gap as C_{60}, so that the mixed nature of our sample should not invalidate our interpretation.

The HREELS visible spectrum comprises ten further peaks or shoulders up to 4 eV. They are listed in Table II, along with data from other spectroscopies. Two peaks are outstanding at 2.2 and 3.7 eV. The latter clearly corresponds to the sharp 329-nm peak observed in the visible-uv absorption spectrum (AS) of thick C_{60} samples,[15,16] as well as in x-ray photoelectron spectroscopy (XPS) (see Table II). The former is absent in AS which, in this energy region, shows only a very weak and broad structure between 450 and 600 nm and does not appear in XPS either. Note that the 2.2 peak has no analog in the C_{70} AS spectrum,[16] which excludes assigning it to this molecule present in our sample as a minority constituent. The other eight visible peaks or shoulders are weaker structures occurring at 1.72, 1.92 (as a shoulder on the 2.20 peak), 2.36, 2.58, 2.74, 3.0, 3.3, and 3.4 eV. The 3-eV peak may possibly correspond to the very sharp but weak peak at 404 nm in AS,[16] while the former three are not seen in AS at all.

Above 4 eV (see Fig. 4), there is one of the largest HREELS peaks at 4.8 eV which definitely correlates with the familiar strong AS band at 260 nm and with the XPS strong peak at the same energy of 4.8 eV. This peak, the two intense HREELS peaks at 2.2 and 3.7, as well as the four nearby weaker structures discussed previously, ex-

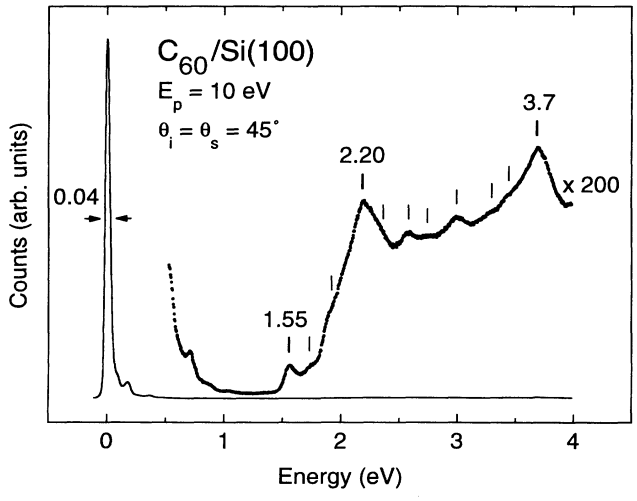

FIG. 3. The near-infrared and visible HREELS spectrum of C_{60}-film/Si(100). Peak positions are indicated by bars and are listed in Table II.

TABLE II. C_{60} visible uv-vuv bands. Comparative list of peak positions (in eV) of visible, uv, and vuv bands observed in four different spectroscopies: HREELS, AS, XPS, and UPS. The strong features are indicated by an asterisk and are represented by a thick line in Fig. 6, which provides a graphical representation of this table.

HREELS[a] *E* (eV)	AS[b] *E* (eV)	XPS[c] *E* (eV)	UPS[d] *E* (eV)
1.55			
1.72			
1.92		1.9	
2.20			
2.36			
2.58			
2.74	2.7		
3.0	3.07		
3.3			
3.4			
3.7*	3.77*	3.7*	
4.8*	4.8*	4.8*	
5.5			
5.8	5.8*	6*	
6.3*			
7.6		7.5*	7.6*
9.4			9.1*
10.2		10	10*
12.8			12.6
14.3			13.6*
		15.6	16*
17.2		18	
28*		28*	
		37	

[a]This work.
[b]References 16 and 17.
[c]Reference 23.
[d]References 22 and 23.

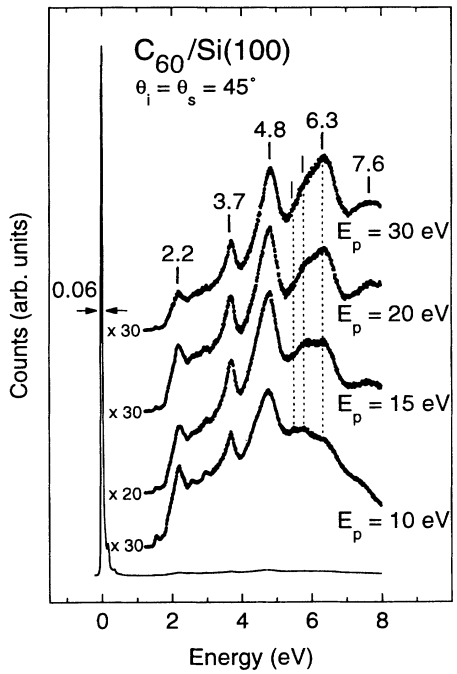

FIG. 4. Set of four HREELS spectra in the visible-uv range for increasing primary-electron energies. Peak positions are listed in Table II.

hibit the very striking property of having relative intensities that remain fairly independent of the primary-electron energy in the wide range from 10 to 50 eV, as shown in the series of spectra of Fig. 4. This is in sharp contrast to the behavior of the next group of intense peaks around 6 eV. It turns out that this group is, in fact, made of three peaks: two peaks of nearly constant intensity at 5.5 eV (225 nm) and 5.8 eV (214 nm) and a third, initially smaller one at 6.3 eV (197 nm) whose intensity grows continuously when the primary electron energy increases above 10 eV. For primary energies above 30 eV, the 6.3-eV peak intensity stabilizes and dominates the 5.8 one which persists as its shoulder. At that point, the 6.3-eV shouldered band strikingly resembles in line shape the corresponding feature observed in AS at 214 nm,[16] notwithstanding the 0.5-eV blueshift of the former with respect to the latter (see below for a discussion of this shift). We argue that, together with the 4.8 peak, the 6.3-eV shouldered band forms the familiar double-peak structure (the so-called camel's-back spectrum) so characteristic of the AS spectrum of C_{60}.[15] This doublet will remain the ubiquitous structure in all further HREELS spectra taken at higher primary-electron energies (see below, Fig. 6). It is instructive to compare the present HREEL spectra in the 6-eV region to the corresponding spectrum of a graphite basal surface.[17,10] In crystalline graphite, there is the so-called π-plasmon peak at about 7- and 2-eV width in the loss function $\mathrm{Im}\epsilon^{-1}$, either directly measured by EELS,[17,18,10] or calculated from synchrotron radiation reflectivity spectra.[19] The peak position shows dispersion[17] but, at small momentum transfers, it occurs precisely at 6.3 eV both in the angle-resolved measurements of Diebold *et al.*[17] and in our own 45° specular reflection measurements on highly oriented pyrolytic graphite. Unlike the present C_{60} double peak, this broad peak is unsplit. It has been interpreted[19] as arising from collective density oscillations of the π-electron system with polarization parallel to the graphite layer. Such oscillations derive from the existence of a group of π to π^* one-electron transitions around 4.5 eV in the band structure of graphite. We suggest that the presently observed HREELS peaks of fixed intensity at 2.2, 3.7, and 4.8 eV (as well as the nearby weaker structures) represent π to π^* one-electron transitions of the C_{60} molecule, whereas the variable-intensity peak at 6.3 eV would be the quantum $\hbar\omega_\pi$ of the collective excitation in the molecular π-electron subsystem.

Is it reasonable to expect that a finite system of 60 π electrons is capable of showing collective density fluctuations similar to those in bulk graphite? Although answering this question will require microscopic calculations of the correlated electronic-response function of the C_{60} molecule, a straightforward macroscopic approach based on Maxwell's equations hints at the likely existence of such collective motions. It can indeed be shown[20] that a rigid transport of the measured graphite dielectric function to a model of the C_{60} molecule consisting of a dielectric spherical shell of finite thickness produces, among other multipolar modes, a triply degenerate $l=1$ ($m=-1,0,+1$) dipolar excitation around 6 eV. These modes can simply be viewed as originating from the π plasmons of wavelength $\lambda=2\pi R\approx 22$ Å of a graphite layer warped into a sphere having the carbon-frame radius R. Whereas these short-wavelength modes are obviously optically inactive in the planar geometry, they become strongly active on the sphere, and can therefore be excited by light absorption (Mie type) as well as by inelastic electron scattering. A sketch of their eigenvectors is shown in Fig. 5.

Granted that these π plasmons exist, why would they show intensity variations according to primary energy? The answer seems to be provided by the long-range nature of dipole scattering and the consequent forward peaking of the inelastic cross section around the specular direction. Indeed, from the dielectric theory of EELS,[7] the half angle of the dipole scattering lobe for π plasmons may be estimated at $\hbar\omega_\pi/2E_p\approx 18°$ for $E_p=10$ eV. Although this theory is quantitatively accurate only for $E_p\gg\hbar\omega_\pi$, this estimate does explain qualitatively the low intensity of the 6.3-eV loss at low primary energy, since most of the inelastically scattered electrons will miss the narrow spectrometer aperture (1.5°). When the electron energy increases, the dipole lobe shrinks down to 6° for $E_p=30$ eV, which results in more electrons being collected and in a gradual increase of the π plasmon-loss peak intensity. A similar effect has been clearly observed in the infrared regime, e.g., for CO molecules adsorbed on Cu(100),[21] and has been quantitatively interpreted along the above lines. The same explanation will be invoked below to understand the observed σ-plasmon variable intensity.

The question remains as to why the peak intensity saturates before the dipole lobe has shrunk down to fully fit

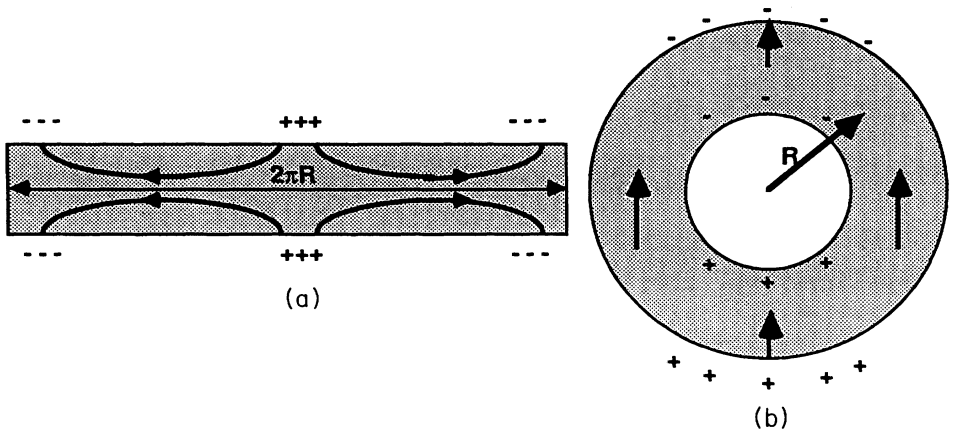

FIG. 5. Sketch of the $pz(l=1, m=0)$ dipole plasmon eigenvector for a spherical dielectric shell (radius R) of finite thickness (b). This mostly tangential mode corresponds to the symmetric mode of wavelength $2\pi R$ in a thin slab (a). The slab antisymmetric mode and the corresponding (mostly radial) shell mode also exist but are not shown. Only the shell modes are optically active (see Ref. 20 for details).

into the spectrometer aperture. A possible explanation is in the diffuse nature of the elastic scattering from our disordered film, as mentioned before. Because of this, the spectrometer will collect not only electrons from the specular beam, but also electrons which have been inelastically scattered by π plasmons away from nearby diffusely scattered beams, namely those beams which are within a conical bundle around the specular beam with an opening again equal to the dipole lobe angle. When the latter shrinks with increasing E_p, the contribution from the outer rays of the diffuse bundle decreases while that of the inner rays increases. Then the net balance and the observed intensity saturation should depend on how fast the diffuse intensity dies down in directions away from the specular beam. Experiments with ordered films should decide whether this interpretation holds true, but one is clearly in need of a quantitative evaluation of the various effects on the basis of an improved version of EELS theory, one which would hold also at low primary-electron energy.

One may further ask why the arguments above do not apply to the one-electron transitions whose strength is observed to remain roughly independent of the primary electron energy above threshold (see Figs. 4 and 6). A nearly constant intensity would result if the one-electron transitions cause more isotropic scattering than the mainly forward scattering on the collective modes. But this is just a consequence of the impact, or short-range nature of the scattering mechanism by individual excitations. The fact remains, however, that there is as yet no theory of impact scattering to verify the quantitative validity of these ideas. Again, clarification of all these questions should be possible by experimenting on ordered films which will eliminate elastic diffuse scattering and for which an off-specular spectrum should reveal only the inelastic-impact-scattering events.[10]

Lastly, the observed 8% blueshift of our HREELS π plasmon at 6.3 eV with respect to the corresponding 5.8-eV feature of the AS double peak can be understood from the different response functions of the two spectroscopies. Basically, AS measures $\mathrm{Im}\epsilon(\omega)$, whereas HREELS (on a thick film) measures $\mathrm{Im}[1+\epsilon(\omega)]^{-1}$. If AS sees a pole in $\epsilon(\omega)$ ($\epsilon=-\infty$) at 5.8 eV, the HREELS loss function will peak at a slightly higher energy given by $\epsilon=-1$. Simulating $\epsilon(\omega)$ with just two Lorentzians for the π-π^* and σ-σ^* transitions corroborates this interpretation quantitatively.[20]

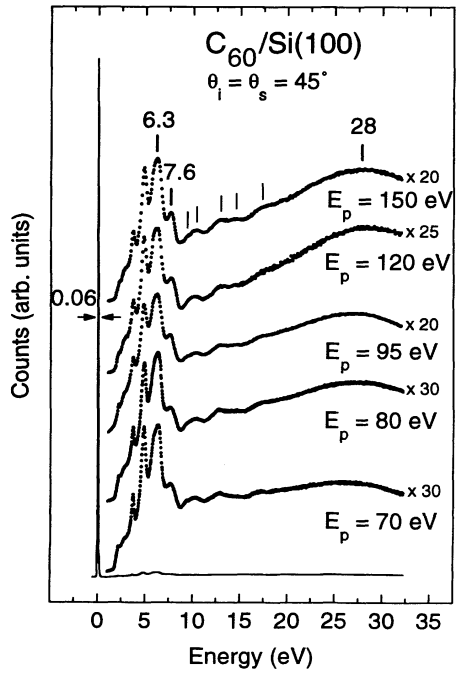

FIG. 6. Set of five HREELS in the uv-vuv for increasing primary-electron energies. Peak positions are listed in Table II.

C. vuv and far vuv

A series of spectra taken with primary-electron energies above 30 eV is shown in Fig. 6. The observed peaks are listed in Table II and Fig. 7. In the vuv, there are six HREELS peaks which remain fairly constant in relative intensity for increasing primary energy. The first peak at 7.6 eV is the strongest and appears to correlate very well with the lowest ionization energy of both the C_{60} gas-phase molecule and of C_{60} thin films on Au foil, as accurately determined by Lichtenberger *et al.*[22] by ultraviolet

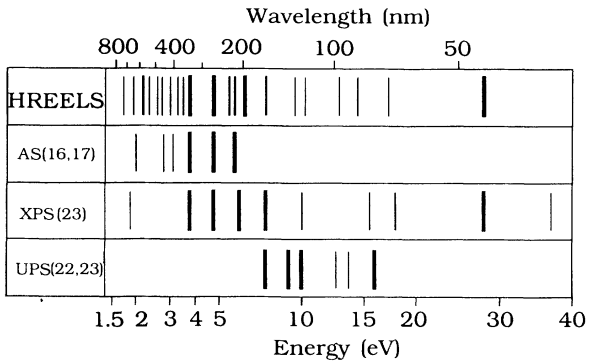

FIG. 7. Peak positions of visible uv-vuv bands of C_{60} (see Table II). The acronyms stand for absorption spectroscopy (AS), x-ray photoelectron spectroscopy (XPS), and ultraviolet photoelectron spectroscopy (UPS). The numbers enclosed in parentheses are references from which data have been taken.

photoemission spectroscopy (UPS). The next five peaks occur at positions closely correlated to UPS lines as observed by using a He source[22] or Synchrotron Radiation by Weaver *et al.*[23] The last peak at 17.2 eV appears to correspond to the 16-eV peak of the He II UPS (also present but weaker in the He I UPS spectrum)[22] and to the 18-eV broadband seen in Synchrotron Radiation UPS and XPS.[23] In general, the HREELS bands in this vuv region do not exactly coincide with the UPS lines; apart from the first ionization level at 7.6 eV, they appear to be shifted by a fraction of an eV. In addition, they are less sharply defined than in the UPS spectra. There are two reasons for this: (i) the optical selection rules of photoelectron spectroscopies do not operate in inelastic electron scattering, and (ii) the HREELS bands are riding over the increasingly intense wing of a broad band centered around 28 eV.

Finally, Fig. 6 illustrates the gradual emergence of this 28-eV broad peak when the primary-electron energy increases beyond 50 eV. We interpret this feature as due to the excitation of incipient σ plasmons, or collective motions of the entire 240 electrons of the valence shell. As a collective excitation, it cannot show up in UPS but it should appear in Synchrotron Radiation AS for photon energies above threshold. In any case, it is clearly detected at just the same position by Weaver *et al.*[23] as a strong shakeup satellite to the XPS C 1*s* core line. The XPS spectrum on the low-energy side of the core line being, in a sense, an EELS spectrum for the C 1*s* ejected electron, it is natural that the peak positions in XPS and HREELS agree quite well. The intensity of the σ plasmons, relative to the 6-eV double peak, which remains fairly unchanged throughout, is seen to grow continuously with increasing primary energy and to saturate around 120 eV.

Microscopic calculations are required to understand the origin of the giant resonance[24] but, again, a simple macroscopic model should help. It can be shown[20] that a spherical dielectric shell of finite thickness possesses two sets of multipolar polarization eigenmodes, basically because the hollow shell has two boundaries. They arise from the interaction of the modes attached to the external boundary (plain-sphere modes) with those attached to the inner boundary (void modes). One set involves mostly tangential charge displacements (the $l=1$ mode is shown in Fig. 5) while the other set consists mostly of radial motions. The eigenmode amplitudes of the two sets are proportional to the spherical harmonics. The two sets correspond, in spherical geometry, to the even and odd eigenmodes of a thin film, respectively. Both tangential and radial dipolar modes ($l=1$) are optically active but the former has at least twice the strength of the latter, depending on the assumed shell thickness. For realistic parameters applicable to the C_{60} shell, the ratio of the strengths is close to 4.[20]

We interpret the 28 HREELS peak as being primarily the $l=1$, triply degenerate eigenmotion of the tangential set for the 240 ($\sigma+\pi$) electrons. Its dipole moment extends along a diameter of the molecule, hence its large oscillator strength. We argue that the gradual increase of its intensity is due to the same long-range dipole scattering and aperture effects as we proposed for the emergence of the π plasmon at 6.3 eV.

Some contributions to the intensity and to the width of this large structure arises from all the other $l\neq 1$ collective, tangential, or radial σ eigenmodes. Their excitation by fast electrons, albeit weaker than the $l=1$ modes, is not forbidden. In particular the $l=0$ radial breathing motion should also contribute, since it has a monopolar coupling to the electron when the latter penetrates the interior of the hollow molecule. Detailed evaluations of the HREELS multipolar-excitation cross sections will be published elsewhere.

Finally, we suggest that the present interpretation of the 28-eV peak, which makes it a purely molecular property rather than a solid-state effect,[23] is consistent with the accepted fact that the fullerites are van der Waals solids in which the intermolecular interactions per molecule are of the order of 1 or 2 eV at most, i.e., negligible as compared to the σ-plasmon quantum.

IV. van der WAALS ENERGY

The van der Waals cohesive energy of C_{60} fullerite can be understood as primarily originating from the ground-state fluctuations of the tangential σ plasmons discussed above via the weak dipole-dipole interactions of neighboring molecules. A qualitative evaluation of this energy goes as follows (see Ref. 20 for a detailed calculation). Let $n=4/a^3$ be the molecule number density in the fcc lattice of parameter a and let $\alpha(\omega)=\alpha(0)/(1-\omega^2/\omega_\sigma^2)$ be a simple Lorentzian model for the σ-electron dynamical polarizability of the C_{60} molecule. Here, for simplicity, we ignore the π plasmons which have a weaker oscillator strength and a smaller zero-point energy. Start from the Clausius-Mossotti formula, which embodies the dipole-dipole interactions in a cubic lattice at long wavelengths: $\epsilon(\omega)=(1+2z/3)/(1-z/3)$, where $z(\omega)=4\pi n\alpha(\omega)$. The zero of $\epsilon(\omega)$ gives the frequency $\omega_L=\omega_\sigma(1+2z_0/3)^{1/2}$ of the longitudinal-polarization eigenmodes of long wavelengths in the solid, while the pole of $\epsilon(\omega)$ provides the doubly degenerate frequency $\omega_T=\omega_\sigma(1-z_0/3)^{1/2}$ of

transverse modes, where $z_0=4\pi n\alpha(0)$. We neglect the dispersion of the polarization waves for finite k in the Brillouin zone. Then the van der Waals energy per molecule is given by the shift in zero-point energy of the above three modes on going from the equilibrium value of a to infinite a: $W=(\hbar/2)(\omega_L+2\omega_T-3\omega_\sigma)$. We use $a=14$ Å and $\alpha(0)\approx 64$ Å^3, considering that the C_{60} molecule has the static polarizability equivalent to that of a metallic shell of outer radius ≈ 4 Å (i.e., about 1 Å^3 per C atom, a value close to the best theoretical estimate of 65 Å^3 obtained by Fowler, Lazaretti, and Zanasi[25]). This gives $z_0=1.17$. We choose $\hbar\omega_\sigma=25.6$ eV for which the surface loss function $-\mathrm{Im}[1+\epsilon(\omega)]^{-1}$ peaks at the observed $\hbar\omega_\sigma(1+z_0/6)^{1/2}=28$ eV. With these parameters, one finds $W=-1.33$ eV. This constitutes a major piece of the cohesive energy evaluated at -1.6 eV by using the local-density approximation[14] and at -1.9 eV by using empirical pair potentials.[26] The pair contribution to the energy in our simple σ-plasmon model is the first nonvanishing term in the expansion of W in powers of z_0,[27] namely, $W_p=-(\hbar\omega_\sigma/2)z_0^2/12\approx -1.46$ eV. When compared to the exact result, this value indicates that many-body effects[27] are not negligible and can make a 10% antibonding contribution to the cohesion of this material. Note that neglecting the dispersion of the polarization waves overestimates the dipolar van der Waals attraction,[27] but further binding contributions should arise from the multipolar π and σ plasmons of higher l's discussed before. These effects can be evaluated by computing the full dispersion relations of the (multi)polarization waves throughout the Brillouin zone.[20]

Note added. Since the submission of the present paper, a number of publications have appeared in the literature to which we want to refer, as they report data similar to those presented here. EELS results on C_{60} films have been obtained by Sohmen *et al.*,[28] Hansen *et al.*,[29] Saito *et al.*,[30] and in the gas phase by Keller *et al.*[31] An empirical thin-spherical-shell model has been constructed by Barton *et al.*[32] with which several theoretical predictions are made concerning the collective behavior of the valence electrons in the C_{60} molecules. Some of these predictions receive support from the data of the present work. Finally, a short version of the present paper has appeared in Ref. 33.

ACKNOWLEDGMENTS

This work was funded by the Belgian national program of Interuniversity Research Projects initiated by the State Prime Minister Office (Science Policy Programming) and by the Belgian National Science Foundation.

[1]H. W. Kroto, J. R. Heath, S. C. O'Brien, R. F. Curl, and R. E. Smalley, Nature (London) **318**, 162 (1985).

[2]W. Krätschmer, L. D. Lamb, K. Fostiropoulos, and D. R. Huffman, Nature (London) **347**, 354 (1990).

[3]Mort La Brecque, Mosaic **22** (1), 40 (1991).

[4]A. A. Lucas and M. Sunjic, Prog. Surf. Sci. **2**, 75 (1972); H. Rather, *Excitations of Plasmons and Interband Transitions by Electrons* (Springer-Verlag, Berlin, 1980); H. Ibach and D. L. Mills, *Electron Energy Loss Spectroscopy and Surface Vibrations* (Academic, New York, 1982).

[5]D. S. Bethune, G. Meijer, W. C. Tang, H. J. Rosen, W. G. Golden, H. Seki, C. A. Brown, and M. S. Devries, Chem. Phys. Lett. **179**, 183 (1991).

[6]R. L. Cappelletti, J. R. D. Copley, W. A. Kamitakahara, Fand Li, J. S. Lannin, and D. Ramage, Phys. Rev. Lett. **66**, 3261 (1991).

[7]R. F. Willis, A. A. Lucas, and G. D. Mahan, in *The Chemical Physics of Solid Surfaces and Heterogeneous Catalysis,* edited by D. A. King and D. P. Woodruff (Elsevier, Amsterdam, 1983), Vol. 2, p. 59.

[8]C. Oshima, T. Aizawa, R. Souda, Y. Ishizawa, and Y. Sumiyoshi, Solid State Commun. **65**, 1601 (1988); T. Aizawa, R. Souda, S. Otani, Y. Ishizawa, and C. Oshima, Phys. Rev. Lett. **64**, 768 (1990).

[9]W. A. Kamitakahara, J. S. Lannin, R. L. Cappelletti, J. R. D. Copley, and F. Li (unpublished).

[10]G. Gensterblum *et al.*, J. Phys. Chem. Solids (to be published).

[11]M. B. Jost, N. Troullier, D. M. Poirier, J. L. Martins, J. H. Weaver, L. P. F. Chibante, and R. E. Smalley, Phys. Rev. B **44**, 1966 (1991); J. L. Martins, N. Troullier, and J. H. Weaver, Chem. Phys. Lett. **180**, 457 (1991).

[12]A. A. Lucas and M. Sunjic, Phys. Rev. Lett. **26**, 229 (1971); in *Progress in Surface Science,* edited by S. G. Davison (Pergamon, New York, 1972), Vol. 2, p. 75.

[13]J. W. Mintmire, B. I. Dunlap, D. W. Brenner, R. C. Mowrey, and C. T. White, Phys. Rev. B **43**, 14 281 (1991); B. I. Dunlap, D. W. Brenner, J. W. Mintmire, R. C. Mowrey and C. T. White, J. Phys. Chem. **95**, 8737 (1991), and references therein.

[14]S. Saito and A. Oshiyama, Phys. Rev. Lett. **66**, 2637 (1991).

[15]W. Krätschmer, K. Fostiropoulos, and D. R. Huffman, Chem. Phys. Lett. **170**, 167 (1990).

[16]J. P. Hare, H. W. Kroto, and R. Taylor, Chem. Phys. Lett. **177**, 394 (1991).

[17]U. Diebold *et al.*, Surf. Sci. **197**, 430 (1988).

[18]K. Zeppenfeld, Z. Phys. **211**, 391 (168).

[19]R. Klucker (unpublished).

[20]Ph. Lambin, A. A. Lucas, and J. P. Vigneron, Phys. Rev. B (to be published).

[21]S. Anderson, B. N. J. Persson, T. Gustafsson, and E. W. Plummer, Solid State Commun. **34**, 473 (1980).

[22]D. L. Lichtenberger, K. W. Nebesny, Ch. D. Ray, D. R. Huffman, and L. D. Lamb, Chem. Phys. Lett. **176**, 203 (1991).

[23]J. H. Weaver, J. L. Martins, T. Komeda, Y. Chen, T. R. Ohno, G. H. Kroll, N. Troullier, R. E. Haufler, and R. E. Smalley, Phys. Rev. Lett. **66**, 1741 (1991).

[24]G. F. George, A. Bulgac, D. Tománek, and Y. Wang, Phys. Rev. Lett. **67**, 2690 (1991).

[25]P. W. Fowler, P. Lazaretti, and R. Zanasi, Chem. Phys. Lett. **165**, 79 (1990).

[26]Y. Guo, N. Karasawa, and W. A. Goddard III, Nature **351**,

464 (1991).
[27]A. A. Lucas, Physica **35**, 353 (1967).
[28]E. Sohmen *et al.*, Europhys. Lett. **17**, 51 (1992).
[29]P. L. Hansen *et al.*, Chem. Phys. Lett. **181**, 367 (1991).
[30]Y. Saito *et al.*, Jpn. J. Appl. Phys. **30**, L1068 (1991).
[31]J. W. Keller *et al.* (unpublished).
[32]G. Barton *et al.*, J. Chem. Phys. **95**, 1512 (1991).
[33]G. Gensterblum *et al.*, Phys. Rev. Lett. **67**, 2171 (1991).

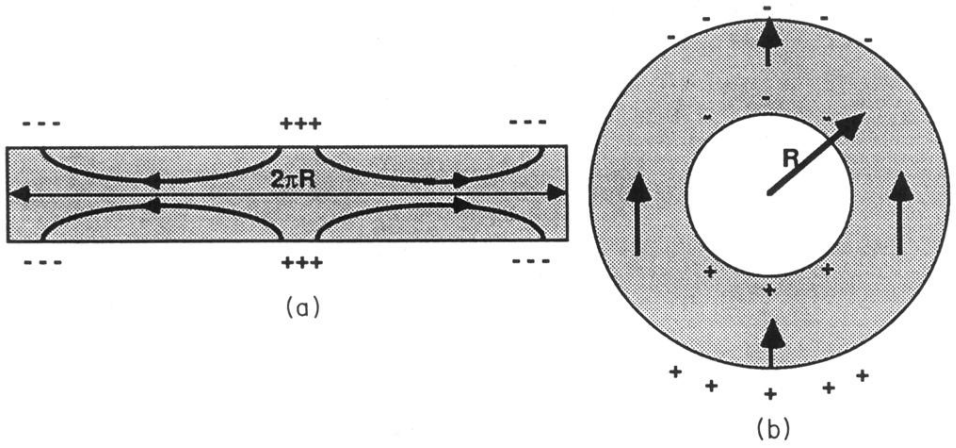

FIG. 5. Sketch of the $pz(l=1, \quad m=0)$ dipole plasmon eigenvector for a spherical dielectric shell (radius R) of finite thickness (b). This mostly tangential mode corresponds to the symmetric mode of wavelength $2\pi R$ in a thin slab (a). The slab antisymmetric mode and the corresponding (mostly radial) shell mode also exist but are not shown. Only the shell modes are optically active (see Ref. 20 for details).